Vol 15 No 9, September 2006
1009-1963/2006/15(09)/1987-09

Chinese Physics

© 2006 Chin. Phys. Soc.
and IOP Publishing Ltd

Forward–backward multiplicity correlations in 4.5 A GeV/c ^{16}O–emulsion interactions*

Zhang Dong-Hai(张东海), Zhao Hui-Hua(赵惠华), Liu Fang(刘 芳), He Chun-Le(何春乐), Jia Hui-Ming(贾会明), Li Xue-Qin(李雪琴), Li Zhen-Yu(李振宇), and Li Jun-Sheng(李俊生)

Institute of Modern Physics, Shanxi Teachers' University, Linfen 041004, *China*

(Received 29 November 2005; revised manuscript received 7 May 2006)

A detailed study of the mechanisms of the emissions of pions and protons in the forward and backward hemispheres in 4.5 A GeV/c oxygen-emulsion interactions has been carried out. The correlations between the multiplicities of secondary charged particles in the backward and forward hemispheres are investigated.

Keywords: relativistic heavy-ion collision, backward–forward correlation, nuclear emulsion
PACC: 2570N, 2940R

1. Introduction

Over the last few years, the production of forward–backward particles in hadron–nucleus and nucleus–nucleus interactions at relativistic energies has received considerable experimental and theoretical attention.[1−5] The study of the emission of relativistic hadrons (mainly pions) from nuclei in the backward direction is important because in the free nucleon–nucleon collisions such production is kinematically restricted, the emission of hadrons beyond the kinematic limit may be an evidence for exotic production mechanisms like production from clusters. Therefore, the emission of such hadrons in heavy ion collisions in the backward hemisphere can supply interesting information on nuclear effects such as the interaction of hadrons from the primary interaction zone with the surrounding nuclear matter, the motion of internal nucleons inside the nucleus, and short range correlation between nucleons. The simple Fermi motion could not account for such backward hadron emission, the dominant mechanism for such production was an interaction between incident nucleons from the projectile and multinucleon clusters in the target (cumulative production).[6−8]

The target nucleus, being an extended object, gives a unique opportunity for studying the space–time evolution of the multiparticle production process. It is useful to analyse the features of the correlations between multiplicities of the shower particles emitted in the forward and backward hemispheres. The backward emissions of protons and pions in the case of hadron–nucleus and nucleus–nucleus interactions have been investigated[5,9−17] and it is found that the backward emission of pions is consistent with the cumulative effect.

In view of this we report here a detailed study on the production of pions and protons in forward and backward hemispheres in the interaction of ^{16}O nuclei with photoemulsion at 4.5 A GeV/c.

2. Experimental details

Stacks of NIKFI BR-2 nuclear emulsion were exposed to a 4.5 A GeV/c oxygen beam at the Joint Institute for Nuclear Research (JINR), Dubna, Russia. The volume of the stacks was 10cm×10cm×0.06cm. Along the track double scanning, fast in the forward direction and slow in the backward direction, was carried out. A total 2960 interactions of oxygen with the nuclei of the emulsion were observed by following a primary track length of 35768.9cm, which led to a mean free path $\lambda = (12.08 \pm 0.22)$cm. From among these interactions, 152 events were found to be pro-

*Project supported by the National Natural Science Foundation of China (Grant No 10475054), the Major Science and Technology Foundation of Ministry of Education of China (Grant No 205026), the Natural Science Foundation of Shanxi Province, China(Grant No 20021007) and Shanxi Provincial Foundation for Returned Scholars of China(Grant No 20031046).

duced by electromagnetic interactions and 149 events were due to elastic interactions. Out of these 2960 interactions, 2044 inelastic interactions were picked up, without any bias, for the final analysis. Interactions that were within 30μm from the top or bottom surface of the emulsion were not taken into consideration for the final analysis.

In the scanning we excluded the events without a formation of charged secondary particles (scattering at small angles without any indications of excitation or breakup of the target nucleus which satisfy the kinematics of an elastic nucleus–nucleus collision) and also the events of electromagnetic nature (production of δ-electrons and e^+, e^- pairs).

The secondary particles in each event are classified according to traditional emulsion terminology into:

i) Shower particles, which are single charged relativistic particles with relative ionization $I/I_0 < 1.4$ where I_0 is the plateau ionization for single charged minimum ionizing particles. They are mainly due to the produced charged pions having a relative speed $\beta = v/c \geq 0.7$. Their multiplicity is denoted by n_s (not including that of the stripped projectile protons).

ii) Grey particle tracks, which are those tracks having a range $R > 3$ mm in emulsion and relative ionization $I/I_0 > 1.4$. They are mostly due to protons with kinetic energies ranging from 26 to 400 MeV. The multiplicity of these grey tracks is denoted by n_g.

iii) Black particle tracks, which are those having a short range in emulsion, $R \leq 3$ mm (corresponding to proton kinetic energy < 26 MeV). Their multiplicity is denoted by n_b. Grey and black tracks together are usually considered as heavily ionizing particles. Their multiplicity is denoted by $n_h = n_g + n_b$.

iv) Any other charged particles, which are emitted at an angle $\theta \leq 3^\circ$ with respect to the incident direction and characterized by no change in its ionization for at least 2 cm from the interaction point. And these particles are regarded as noninteracting (stripped) projectile fragments (PFs).

The shower tracks in each event that were emitted in the backward hemisphere (i.e. $90^\circ \leq \theta \leq 180^\circ$) are called backward shower particles. The multiplicity of this type of tracks in each event is denoted by n_s^b. The multiplicity of shower particles emitted in the forward hemisphere ($\theta < 90^\circ$) in each event is denoted by n_s^F, where $n_s = n_s^b + n_s^F$. Also, for the grey tracks $n_g = n_g^b + n_g^F$, and for the black tracks $n_b = n_b^b + n_b^F$.

3. Experimental results

The study of the hadron–nucleus and nucleus–nucleus interactions may provide valuable information about the multi-particle production mechanism and the space–time evolution of the considered reactions.[18−25] The nuclear emulsion, serving as a 4π-detector, is suitable for detecting all the charged particles emitted in the whole space. The interaction of a high energy hadron or nucleus with a target nucleus occurs through two main steps. One is very rapid, having a time almost equal to the time taken by light to cross the target nucleus. During this step, fast particles or intermediate systems (which decay immediately to fast particles, e.g. strings, plasma, cluster, etc.) are produced. The produced intermediate systems or the fast particles may collide with a target nucleon or more before decaying. The struck nucleons recoil and may leave the target nucleus. Thus, the hadron–nucleus or nucleus–nucleus interactions can be viewed as a cascade of hadron–nucleon collisions. In emulsion physics, fast charged particles with a speed $\beta(= v/c) > 0.7$ are called 'shower' particles. The charged recoil nuclei emitted from the target nucleus with $0.3 \leq \beta \leq 0.7$ are referred to as 'grey' particles. At the end of the first step, the residual target nuclei are left in a highly excited state of high temperature. The others start and last a relatively long time. During this period, the excited residual nuclei attain thermal equilibrium and lose their excitation energies by evaporation processes, i.e. by emitting slow nucleons and nuclear fragments. The emitted slow charged particles are called 'black' particles.

Multiplicity distributions of shower and grey tracks in the forward and backward hemispheres, produced in ^{16}O-Em interactions at 4.5 A GeV/c, are shown in Figs.1 and 2. For comparison, the results from the interactions of carbon and silicon with emulsion at the same energy are also presented in the figures. From these figures the multiplicity distributions of shower and grey particles in the backward hemisphere are observed to be similar to those for the compared projectiles, which means that the particle production in the backward hemisphere is independent of the projectile mass. However, in the forward hemisphere the distributions tend to become broader with the increase of projectile mass, which is the same as the result in Refs.[26] or [27]. It is shown in Ref.[1] or [28] that the value of $\langle n_s^F \rangle$ is proportional to the average number of interacting nucleons from each pro-

jectile $\langle N_{\rm int}\rangle$ with emulsion nuclei, which supports the idea of considering the nucleus–nucleus collisions as a superposition of nucleon–nucleus collisions, while the value of $\langle n_{\rm s}^{\rm b}\rangle$ is nearly independent of $\langle N_{\rm int}\rangle$.

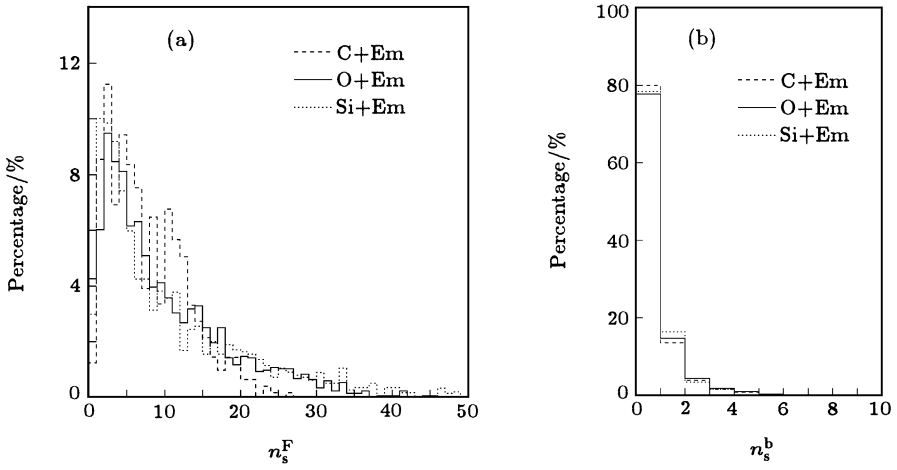


Fig.1. Multiplicity distributions of shower particles in the forward $n_{\rm s}^{\rm F}$ (a) and backward $n_{\rm s}^{\rm b}$ (b) hemispheres.

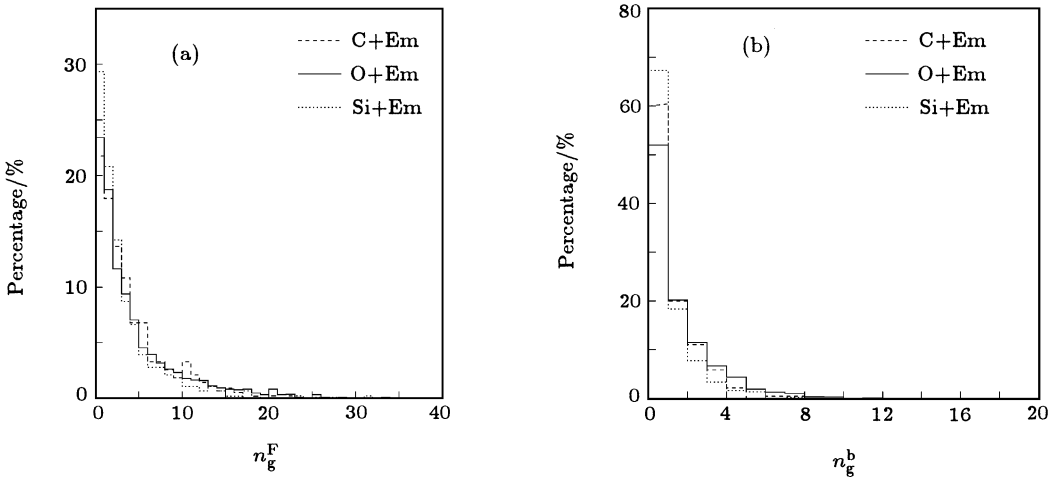


Fig.2. Multiplicity distributions of grey particles in the forward $n_{\rm g}^{\rm F}$ (a) and backward $n_{\rm g}^{\rm b}$ (b) hemispheres.

Table 1 shows the values of average multiplicities of shower and grey particles in the forward and backward hemispheres, the forward–backward ratio, and the $\langle N_{\rm int}\rangle$. The average multiplicities of shower and grey particles listed in Table 1 indicate that the probability of the forward emission is much higher than that for the backward emission. This fact is also reflected in the value of forward–backward ratio. The data in this table also show a significant increase in value of $\langle n_{\rm s}^{\rm b}\rangle$ as the number of incident projectile increases up to the mass number of ^{7}Li. The values of $\langle n_{\rm s}^{\rm b}\rangle$ within experimental error are nearly equal in the interactions induced by ^{7}Li, ^{12}C, ^{16}O, ^{22}Ne, ^{28}Si and ^{32}S nuclei. On the other hand, the value of the average multiplicity of shower particles produced in the forward hemisphere, $\langle n_{\rm s}^{\rm F}\rangle$, are strongly dependent on the projectile size (i.e. dependent on the average number of interacting projectile nucleons, $\langle N_{\rm int}\rangle$). As the projectile size increases, a great number of projectile nucleons interact with the target nucleons. It is observed that the value of the shower particles emitted in the backward hemisphere is nearly constant within the experimental error for projectile of mass number being larger than or equal to 7. This means that the creation of shower particles in the backward hemisphere is nearly independent of the projectile mass number at a similar momentum per nucleon.

Table 1. The average multiplicities of shower and grey particles in the forward and backward hemispheres, the forward–backward ratio, and $\langle N_{\rm int}\rangle$.

Beam	$\langle n_{\rm s}^{\rm F}\rangle$	$\langle n_{\rm s}^{\rm b}\rangle$	$\langle n_{\rm g}^{\rm F}\rangle$	$\langle n_{\rm g}^{\rm b}\rangle$	$\langle N_{\rm int}\rangle$	$\langle F/B\rangle_{\rm s}$	$\langle F/B\rangle_{\rm g}$	Ref.
p	1.50 ± 0.01	0.11 ± 0.02	0.03 ± 0.02		1.0	13.16		[1]
^{4}He	4.04 ± 0.01	0.23 ± 0.01	0.24 ± 0.04		2.42	17.56		[1]
^{6}Li	5.30 ± 0.15	0.41 ± 0.01	2.08 ± 0.08	0.98 ± 0.05	3.56	13.83	2.15	[29]
^{7}Li	4.96 ± 0.03	0.40 ± 0.01	3.68 ± 0.20	0.94 ± 0.04	3.92	12.15	3.92	[30]
^{12}C	7.11 ± 0.02	0.42 ± 0.01	4.52 ± 0.20	1.38 ± 0.07	5.28	16.93	3.51	[1]
	7.38 ± 0.19	0.29 ± 0.03	4.83 ± 0.19	1.10 ± 0.06		25.39	4.39	[5]
^{16}O	10.03 ± 0.30	0.46 ± 0.02	3.58 ± 0.15	0.97 ± 0.04	6.35	21.74	3.69	[28]
	9.84 ± 0.19	0.38 ± 0.02	4.47 ± 0.13	1.22 ± 0.04	7.65	25.89	3.67	this work
^{22}Ne	9.85 ± 0.04	0.45 ± 0.01	4.80 ± 0.20	1.42 ± 0.08	8.06	21.89	3.30	[1]
	9.71 ± 0.23	0.40 ± 0.02				24.27		[2]
^{28}Si	11.36 ± 0.09	0.44 ± 0.02	4.98 ± 0.18	1.42 ± 0.07	9.49	25.82	3.52	[1]
	10.95 ± 0.31	0.29 ± 0.02	7.34 ± 0.13	1.43 ± 0.03		37.76	5.13	[5]
^{32}S	14.58 ± 0.48	0.46 ± 0.03	3.17 ± 0.14	0.82 ± 0.05	14.68	31.76	3.91	[29]

The correlation between the multiplicities of different types of particles emitted in the backward and forward hemisphere is one of the most sensitive sources of information about the mechanisms of particle production in both forward and backward hemispheres. Figure 3 presents the correlations of $\langle n_{\rm s}^{\rm F}(n_{\rm s}^{\rm b})\rangle$, $\langle n_{\rm g}^{\rm F}(n_{\rm s}^{\rm b})\rangle$ and $\langle n_{\rm b}^{\rm F}(n_{\rm s}^{\rm b})\rangle$ with $n_{\rm s}^{\rm b}$ (a), and those of $\langle n_{\rm s}^{\rm b}(n_{\rm s}^{\rm F})\rangle$, $\langle n_{\rm g}^{\rm b}(n_{\rm s}^{\rm F})\rangle$ and $\langle n_{\rm b}^{\rm b}(n_{\rm s}^{\rm F})\rangle$ with $n_{\rm s}^{\rm F}$ (b) for ^{16}O-Em interactions at 4.5 A GeV/c respectively. The experimental data are fitted by a linear relation as follows for $\langle n_{\rm s}^{\rm F}(n_{\rm s}^{\rm b})\rangle$ and $n_{\rm s}^{\rm b}$, and, $\langle n_{\rm s}^{\rm b}(n_{\rm s}^{\rm F})\rangle$ and $n_{\rm s}^{\rm F}$:

$$\langle n_{\rm s}^{\rm F}\rangle = a_{\rm F} + b_{\rm F} n_{\rm s}^{\rm b}, \tag{1}$$

$$\langle n_{\rm s}^{\rm b}\rangle = a_{\rm B} + b_{\rm B} n_{\rm s}^{\rm F}. \tag{2}$$

The values of $b_{\rm F}$ and $b_{\rm B}$ are listed in Table 2. For comparison, the results from other projectiles induced nuclear emulsion reactions are also presented in the table. From the analyses of Fig.3 and Table 2, it may be noticed that a strong correlation between $\langle n_{\rm s}^{\rm F}\rangle$ and $n_{\rm s}^{\rm b}$ can be seen, but between $\langle n_{\rm s}^{\rm b}\rangle$ and $n_{\rm s}^{\rm F}$, the correlation is not so strong. Also, from the table one may notice that $b_{\rm F}$ increases with the increase of the projectile mass, which means that $\langle n_{\rm s}^{\rm F}\rangle$ increases with the projectile mass number while $\langle n_{\rm s}^{\rm b}\rangle$ remains nearly constant within experimental error. This is due to the fact that the average number of all shower particles depends on the number of the interacting nucleons from projectile. Since the shower particles are very fast, they are emitted mainly in the forward direction in the laboratory system.

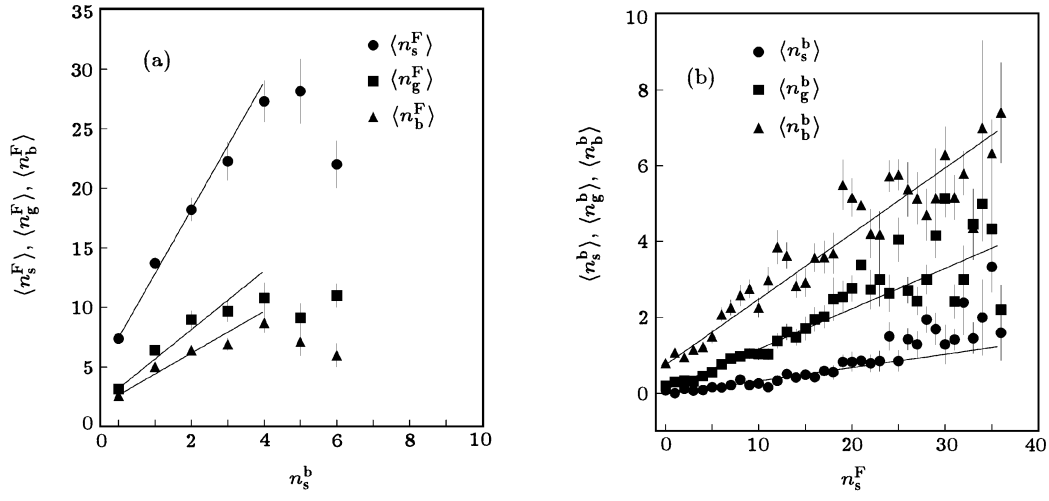


Fig.3. The correlations of $\langle n_{\rm s}^{\rm F}\rangle$, $\langle n_{\rm g}^{\rm F}\rangle$ and $\langle n_{\rm b}^{\rm F}\rangle$ with $n_{\rm s}^{\rm b}$ (a), and those of $\langle n_{\rm s}^{\rm b}\rangle$, $\langle n_{\rm g}^{\rm b}\rangle$ and $\langle n_{\rm b}^{\rm b}\rangle$ with $n_{\rm s}^{\rm F}$ (b) respectively.

Table 2. The values of forward–backward correlation coefficient for ^{16}O-Em interactions at 4.5 A GeV/c and the corresponding results from other nuclei induced emulsion interactions.

Projectile	Momentum	b_{F}	b_{B}	Ref.
^{7}Li	3 A GeV/c	3.18 ± 0.15	0.032 ± 0.001	[16],[30]
^{12}C	4.5 A GeV/c	4.83 ± 0.67		[3]
^{16}O	4.5 A GeV/c	5.37 ± 0.25	0.035 ± 0.003	this work
^{22}Ne	4.1 A GeV/c	6.43 ± 0.18	0.029 ± 0.002	[2],[16],[30]
^{22}Ne	4.1 A GeV/c	7.78 ± 0.45		[3]
^{28}Si	4.5 A GeV/c	8.14 ± 0.41	0.017 ± 0.002	[2],[16],[30]
^{28}Si	4.5 A GeV/c	7.68 ± 0.70	0.041 ± 0.003	[5]
^{28}Si	4.5 A GeV/c	8.79 ± 1.02		[3]

Figure 3 also presents the mean multiplicities of grey and black particles emitted in the forward hemisphere as a function of the shower particles produced in backward hemisphere (a), and the relation between the average multiplicities of grey and black particles produced in the backward hemisphere and the values of $n_{\mathrm{s}}^{\mathrm{F}}$ (b). It shows that the values of $\langle n_{\mathrm{b}}^{\mathrm{b}} \rangle$ and $\langle n_{\mathrm{g}}^{\mathrm{b}} \rangle$ increase with the increase of the values of $n_{\mathrm{s}}^{\mathrm{F}}$, the values of $\langle n_{\mathrm{b}}^{\mathrm{F}} \rangle$ and $\langle n_{\mathrm{g}}^{\mathrm{F}} \rangle$ increase linearly with the value of $n_{\mathrm{s}}^{\mathrm{b}}$ increasing up to 4 and then become approximately constant, within experimental error, for $n_{\mathrm{s}}^{\mathrm{b}} > 4$.

The correlation between grey and shower particles is very important due to their mutual dependence on the number of struck nucleons. Moreover, the protons produced in the backward hemisphere are mainly due to inelastic nucleon–nucleon interactions with the subsequent production of pions. Figure 4 shows (a) the correlations between the average multiplicities of shower, grey and black particles produced in the forward hemisphere and the number of grey particles emitted in the backward hemisphere, and (b) the dependences of the mean values of shower, grey and black particles produced in the backward hemisphere on the number of grey particles emitted in the forward hemisphere. It shows that the value of $\langle n_{\mathrm{g}}^{\mathrm{F}} \rangle$ ($\langle n_{\mathrm{g}}^{\mathrm{b}} \rangle$) increases linearly with the increase of $n_{\mathrm{g}}^{\mathrm{b}}$ ($n_{\mathrm{g}}^{\mathrm{F}}$). From the figure one can also see that the values of $\langle n_{\mathrm{s}}^{\mathrm{F}} \rangle$ and $\langle n_{\mathrm{b}}^{\mathrm{F}} \rangle$ increase with the number of backward grey particles increasing up to $n_{\mathrm{g}}^{\mathrm{b}} \approx 4$. This could be due to the fact that in the region of $n_{\mathrm{g}}^{\mathrm{b}} \leq 4$, a superposition of interactions with light and heavy components of emulsion may exist. For higher $n_{\mathrm{g}}^{\mathrm{b}}$ values, an almost constant behaviour is observed. Such a trend can be understood by the process in spectator parts. From $n_{\mathrm{g}}^{\mathrm{b}} > 4$, the interactions with heavy emulsion nuclei are weakly connected with the process of hadronic production (production of shower particle), but for the production of target evaporated fragments it is limited by the volume of target. For the correlations of $\langle n_{\mathrm{s}}^{\mathrm{b}} \rangle$ and $\langle n_{\mathrm{g}}^{\mathrm{b}} \rangle$ with $n_{\mathrm{g}}^{\mathrm{F}}$, the same trend is observed (Fig.4(b)), but the plateaus of $\langle n_{\mathrm{s}}^{\mathrm{b}} \rangle$ and $\langle n_{\mathrm{b}}^{\mathrm{b}} \rangle$ are at about $n_{\mathrm{g}}^{\mathrm{F}} \approx 9$. The different values of $n_{\mathrm{g}}^{\mathrm{F}}$ and $n_{\mathrm{g}}^{\mathrm{b}}$ presented a plateau region may indicate a difference in mechanism between particle production in nucleus–nucleus interactions in the forward hemisphere and that in the backward hemisphere.

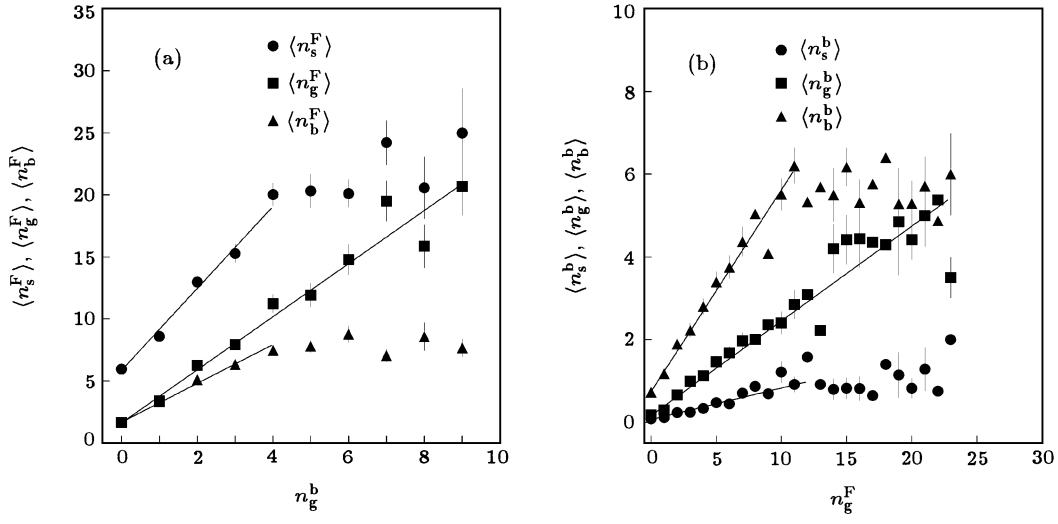


Fig.4. Variations of $\langle n_{\mathrm{s}}^{\mathrm{F}} \rangle$, $\langle n_{\mathrm{g}}^{\mathrm{F}} \rangle$ and $\langle n_{\mathrm{b}}^{\mathrm{F}} \rangle$ with $n_{\mathrm{g}}^{\mathrm{b}}$ (a), and those of $\langle n_{\mathrm{s}}^{\mathrm{b}} \rangle$, $\langle n_{\mathrm{g}}^{\mathrm{b}} \rangle$ and $\langle n_{\mathrm{b}}^{\mathrm{b}} \rangle$ with $n_{\mathrm{g}}^{\mathrm{F}}$ (b).

Figure 5 presents the dependences of $\langle n_s^F\rangle$, $\langle n_g^F\rangle$ and $\langle n_b^F\rangle$ on the number of black particles produced in the backward hemisphere (a), and the dependences of $\langle n_s^b\rangle$, $\langle n_g^b\rangle$ and $\langle n_b^b\rangle$ on the number of black particles emitted in the forward hemisphere (b). We know that the shower particles are related to the excitation energy of nucleus (through the dependence of participant nucleons of the two colliding nuclei on cascade particles) and thus in an indirect way to the evaporated target fragments. From the figure one can see that the dependence of $\langle n_s^F\rangle$ on n_b^b is linear in a region of $n_b^b \leq 8$, which is the same as the dependence of $\langle n_s^b\rangle$ on n_s^F. As shown in the figure, there is a flat region for $n_b^b \geq 8$, which is often referred to as a plateau. This region corresponds to the full overlap of projectile and target nuclei, i.e. to collisions with an impact parameter equal to the difference between two colliding nuclear radii. This type of collision is called a central collision. It exhibits the absence of projectile fragmentation, and emission of a large number of secondary fragments.

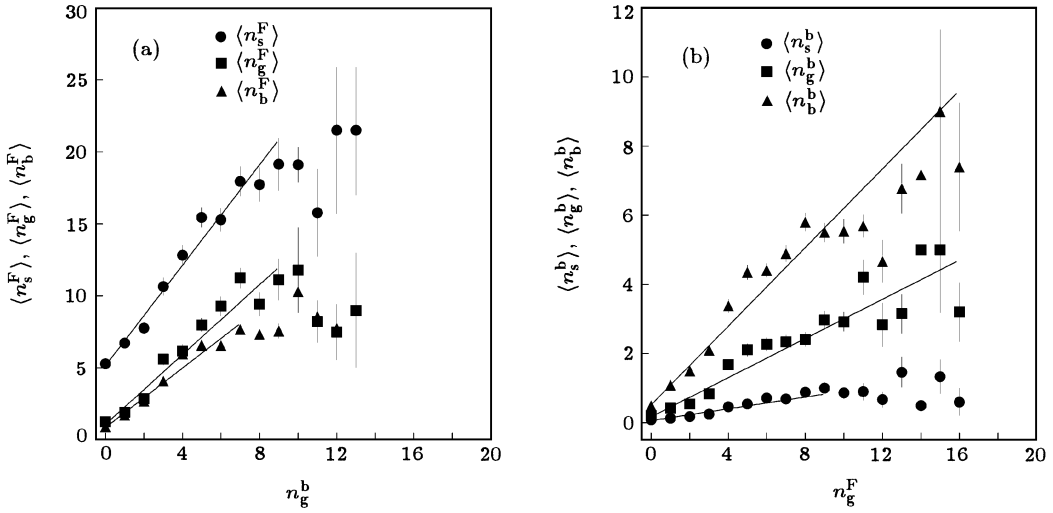


Fig.5. Variations of $\langle n_s^F\rangle$, $\langle n_g^F\rangle$ and $\langle n_b^F\rangle$ with n_b^b (a), and those of $\langle n_s^b\rangle$, $\langle n_g^b\rangle$ and $\langle n_b^b\rangle$ with n_b^F (b).

Figure 6 shows the dependences of forward–backward mean multiplicities of shower and black particles on the number of grey particles. One can see that there is a stronger correlation between $\langle n_s^F\rangle$ and n_g than between $\langle n_s^b\rangle$ and n_g in a region of $n_g \leq 15$. For the black particles emitted in the forward and backward the dependences are the same, which confirms that the mechanisms of the production of black particles in the forward and backward hemispheres are the same.

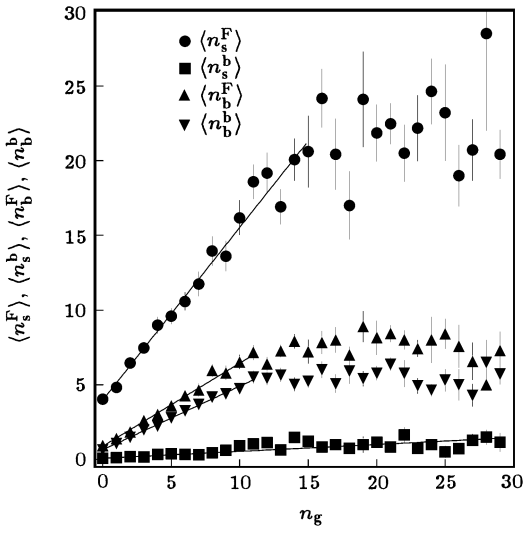


Fig.6. Forward–backward mean multiplicities of shower and black particles as a function of the number of grey tracks.

The average multiplicities of shower and grey particles emitted in the forward and backward hemispheres as a function of the number of black particles are plotted in Fig.7. The linear dependence is also found.

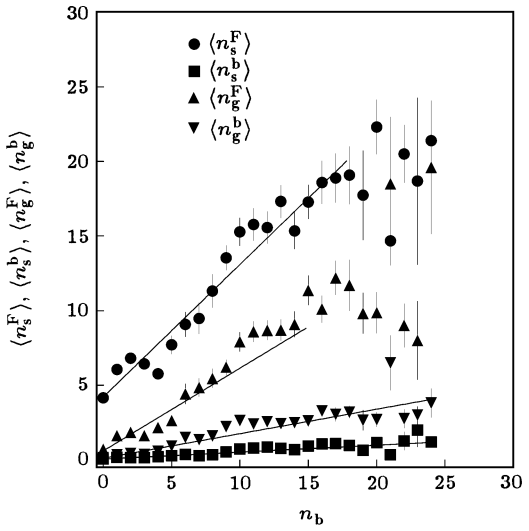


Fig.7. Forward–backward mean multiplicities of shower and grey particles as a function of the number of black tracks.

It is known that the impact parameter is difficult to measure experimentally. We consider the multiplicity of target fragments as a measure of the impact parameter. The higher the value of n_h, the lower the impact parameter, and vice versa. In Fig.8, we study the dependences of the mean multiplicities of shower, black, and grey particles emitted in the forward and backward hemispheres on the number of target fragments (n_h). It is seen that the values $\langle n_s^F \rangle$ and $\langle n_s^b \rangle$ increase linearly with n_h up to 30 and become approximately constant within experimental error for $n_h > 30$. The increase of $\langle n_s^b \rangle$ with n_h is slower than that of $\langle n_s^F \rangle$. The dependences of the average number of grey particles emitted in the forward and backward hemispheres on n_h become stronger with the increase of n_h, i.e. with the decrease of impact parameter. Also, at $n_h \approx 8$ there are the separations of the interactions that are mostly with light nuclei from those with heavy ones. In peripheral nucleus–nucleus interactions, the de-excitation of the residual nuclei proceeds via evaporation of nucleons and light fragments until a stable configuration is reached. In Fig.8 we can also see that n_h increasing from 0 to 25 is accompanied by an increase in the multiplicity of black particles. This is due to the superposition of the characteristics of two groups of events with the small and large multiplicities of black particles.

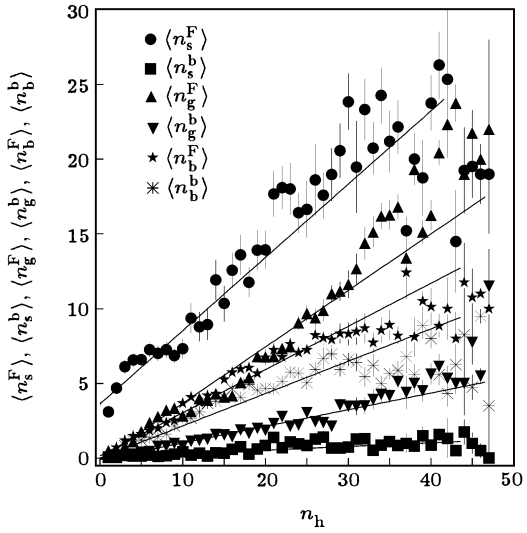


Fig.8. Forward–backward mean multiplicities of shower, grey and black particles as a function of the number of heavily ionizing particles.

All of the possible multiplicity correlations in the previous figures are fitted by a linear relation in the form

$$\langle n_i^{F,b} \rangle = a n_j + b, \tag{3}$$

where $\langle n_i^{F,b} \rangle$ means the mean multiplicities of shower, grey, and black particles emitted in the forward and backward hemispheres, and n_j is the number of different particles. The values of the slope and intercept parameters (a and b) for all possible correlations are given in Table 3. For comparison, the results from other experiments[5,29] are also presented in the table. From the results in the table and previous figures, the following conclusions can be drawn. (i) The average numbers of shower, grey, and black particles in the forward and backward hemispheres increase with the increase of values of n_b and n_h. For $\langle n_s^F \rangle$ and $\langle n_s^b \rangle$ these dependences become stronger with the increase of projectile mass. (ii) The average multiplicities of shower and black particles emitted in the forward and backward hemispheres increase with the increase of the number of grey particles. For shower particles the forward correlation is stronger than the backward one, but for black particle the dependences are the same for the backward and forward production. (iii) The average values of shower and grey particles in the forward hemisphere depend strongly on the number of grey and shower particles in the backward hemisphere. However, the average numbers of grey and shower particles in the backward hemisphere depend weakly on the numbers of shower and grey particles emitted in the forward hemisphere respectively.

This shows that the pions and protons produced in the backward hemisphere are somewhat different from those emitted in the forward hemisphere. The dependences of $\langle n_{\rm s}^{\rm F}\rangle$, respectively, on the numbers of shower and grey particles emitted in the backward hemisphere become stronger with the increase of projectile mass, and the same dependence for $\langle n_{\rm s}^{\rm b}\rangle$ is also observed. (iv) The forward–backward multiplicity correlation is more pronounced in the case of pions than in the case of protons. (v) The mean multiplicities of shower, grey, and black particles produced in the forward and backward hemispheres depend linearly on the numbers of black particles emitted in the forward and backward hemisphere respectively. (vi) The forward–backward multiplicity correlations are stronger than the backward–forward ones.

Table 3. The fitting parameters of the slope and the intercept in the possible forward and backward multiplicity correlations using linear relation Eq.(3).

Correlation	^{16}O-Em		^{28}Si-Em[5]		^{32}S-Em[29]	
	Slope	Intercept	Slope	Intercept	Slope	Intercept
$\langle n_{\rm s}^{\rm F}\rangle$-$n_{\rm h}$	$.49 \pm .01$	$3.63 \pm .11$	$.726 \pm .012$	$2.383 \pm .254$	$.76 \pm .03$	$5.64 \pm .62$
$\langle n_{\rm g}^{\rm F}\rangle$-$n_{\rm h}$	$.378 \pm .005$	$-0.12 \pm .03$	$.290 \pm .009$	$-0.018 \pm .154$	$.28 \pm .02$	$-0.25 \pm .44$
$\langle n_{\rm b}^{\rm F}\rangle$-$n_{\rm h}$	$.289 \pm .004$	$0.16 \pm .03$			$.38 \pm .02$	$-0.48 \pm .38$
$\langle n_{\rm s}^{\rm b}\rangle$-$n_{\rm h}$	$.025 \pm .002$	$0.019 \pm .011$	$.034 \pm .001$	$-0.010 \pm .014$	$5.20 \pm .04$	$-0.15 \pm .07$
$\langle n_{\rm g}^{\rm b}\rangle$-$n_{\rm h}$	$.111 \pm .003$	$-0.096 \pm .016$	$.076 \pm .002$	$-0.123 \pm .052$	$8.43 \pm .01$	$-0.17 \pm .08$
$\langle n_{\rm b}^{\rm b}\rangle$-$n_{\rm h}$	$.216 \pm .003$	$-0.007 \pm .019$			$.23 \pm .01$	$0.35 \pm .17$
$\langle n_{\rm s}^{\rm F}\rangle$-$n_{\rm b}$	$.89 \pm .03$	$4.20 \pm .16$	$.978 \pm .041$	$3.680 \pm .581$		
$\langle n_{\rm g}^{\rm F}\rangle$-$n_{\rm b}$	$.55 \pm .02$	$.59 \pm .06$	$.449 \pm .021$	$.125 \pm .274$		
$\langle n_{\rm s}^{\rm b}\rangle$-$n_{\rm b}$	$.047 \pm .003$	$.038 \pm .009$	$.051 \pm .002$	$-0.019 \pm .029$		
$\langle n_{\rm g}^{\rm b}\rangle$-$n_{\rm b}$	$.164 \pm .006$	$.107 \pm .017$	$.093 \pm .006$	$-0.018 \pm .154$		
$\langle n_{\rm s}^{\rm F}\rangle$-$n_{\rm g}$	$1.16 \pm .04$	$3.96 \pm .14$				
$\langle n_{\rm b}^{\rm F}\rangle$-$n_{\rm g}$	$.56 \pm .02$	$.88 \pm .05$				
$\langle n_{\rm s}^{\rm b}\rangle$-$n_{\rm g}$	$.046 \pm .003$	$.074 \pm .009$				
$\langle n_{\rm b}^{\rm b}\rangle$-$n_{\rm g}$	$.43 \pm .02$	$.64 \pm .04$				
$\langle n_{\rm s}^{\rm F}\rangle$-$n_{\rm s}^{\rm b}$	$5.37 \pm .25$	$7.46 \pm .16$	$7.681 \pm .701$	8.184 ± 1.394		
$\langle n_{\rm g}^{\rm F}\rangle$-$n_{\rm s}^{\rm b}$	$2.47 \pm .17$	$3.21 \pm .11$	$2.116 \pm .506$	3.276 ± 1.367		
$\langle n_{\rm s}^{\rm b}\rangle$-$n_{\rm s}^{\rm b}$	$1.75 \pm .10$	$2.66 \pm .07$				
$\langle n_{\rm s}^{\rm b}\rangle$-$n_{\rm s}^{\rm F}$	$.035 \pm .002$	$-0.026 \pm .008$	$.041 \pm .003$	$-0.121 \pm .052$		
$\langle n_{\rm g}^{\rm b}\rangle$-$n_{\rm s}^{\rm F}$	$.106 \pm .004$	$.101 \pm .025$	$.061 \pm .002$	$-0.023 \pm .048$		
$\langle n_{\rm b}^{\rm b}\rangle$-$n_{\rm s}^{\rm F}$	$.173 \pm .006$	$.751 \pm .053$				
$\langle n_{\rm s}^{\rm F}\rangle$-$n_{\rm g}^{\rm b}$	$3.30 \pm .15$	$5.85 \pm .16$	$4.991 \pm .317$	$7.831 \pm .959$		
$\langle n_{\rm g}^{\rm F}\rangle$-$n_{\rm g}^{\rm b}$	$2.14 \pm .07$	$1.62 \pm .69$	$2.215 \pm .261$	$1.922 \pm .800$		
$\langle n_{\rm b}^{\rm F}\rangle$-$n_{\rm g}^{\rm b}$	$1.57 \pm .06$	$1.67 \pm .06$				
$\langle n_{\rm s}^{\rm b}\rangle$-$n_{\rm g}^{\rm F}$	$.076 \pm .006$	$.068 \pm .012$	$.083 \pm .007$	$.075 \pm .075$		
$\langle n_{\rm g}^{\rm b}\rangle$-$n_{\rm g}^{\rm F}$	$.229 \pm .007$	$.161 \pm .018$	$.139 \pm .014$	$.296 \pm .158$		
$\langle n_{\rm b}^{\rm b}\rangle$-$n_{\rm g}^{\rm F}$	$.49 \pm .02$	$.74 \pm .04$				
$\langle n_{\rm s}^{\rm F}\rangle$-$n_{\rm b}^{\rm b}$	$1.75 \pm .07$	$5.15 \pm .17$				
$\langle n_{\rm g}^{\rm F}\rangle$-$n_{\rm b}^{\rm b}$	$1.21 \pm .04$	$1.07 \pm .07$				
$\langle n_{\rm b}^{\rm F}\rangle$-$n_{\rm b}^{\rm b}$	$1.03 \pm .03$	$.864 \pm .045$				
$\langle n_{\rm s}^{\rm b}\rangle$-$n_{\rm b}^{\rm F}$	$.085 \pm .007$	$.061 \pm .013$				
$\langle n_{\rm g}^{\rm b}\rangle$-$n_{\rm b}^{\rm F}$	$.28 \pm .01$	$.17 \pm .02$				
$\langle n_{\rm b}^{\rm b}\rangle$-$n_{\rm b}^{\rm F}$	$.569 \pm .013$	$.518 \pm .035$				

4. Conclusions

From the exhaustive analyses of the data we conclude as follows.

(i) The multiplicity distributions of shower and grey particles emitted in the backward hemisphere are stable with respect to the projectile mass. This shows that the produced particles in backward hemisphere is independent of the projectile mass.

(ii) The forward–backward multiplicity correla-

tions are observed to be linear. These correlations exhibit that the energy transfer from the target fragmentation by the projectile increases with the increase of the numbers of backward pions and protons.

(iii) The forward production of shower and grey particles is related to the projectile mass.

Acknowledgment

We are thankful to Professor Otterlund I of Lund University in Sweden for supplying the emulsion plates.

References

[1] El-Nadi M, Abdelsalam A and Ali-Mossa N 1994 *Int. J. Mod. Phys.* E **3** 811
[2] El-Naghy A, Sadek N M and Mohery M 1997 *Nuovo Cimento* A **110** 125
[3] El-Nadi M, Ali-Mossa N Abdelsalam A 1997 *Nuovo Cimento* A **110** 1255
[4] El-Nadi M, Abdelsalam A, Ali-Mossa N, Abou-Moussa Z, Kamel S, Abdel-Waged Kh, Osman W and Badawy B 1998 *Eur. Phys. J.* A **3** 183
[5] Ahmad T and Irfan M 1992 *Phys. Rev.* C **46** 1483
[6] Frankfurt L L and Strikman M I 1979 *Phys. Lett.* B **83** 497
[7] Gorenstein M I and Zinovjev G M 1977 *Phys. Lett.* B **67** 100
[8] Mathis H B and Ta-Chung M 1978 *Phys. Rev.* C **18** 952
[9] Andronenko M N, Vol'Nin E N, Vorobev A A, Grachev V T, Lobodenko A A, Strakovskii I I and Uvarov L N 1983 *JETP Lett.* **37** 530
[10] Gavrishchuk O P, Moroz N S, Peresedov V P, Zolin L S, Belyaev I M and Lobanov V V 1991 *Nucl. Phys.* A **523** 589
[11] Aliev SH M, Edgorov S O, Lutpullaev S L, Olimov K, Rasulov N, Rodionova T P, Turdaliev K T and Yuldashev B S 1990 *Sov. J. Nucl. Phys.* **51** 1008
[12] Agababyan N M, Ajinenko I, Ataian M R, Belous K S, Charlet M, Chliapnikov P V, De Wolf E A, Dziunikowska K, Endler A M, Garutchava Z C, Gulkanian H R, Hakobyan R S, Karamian J K, Kisielewska D, Kittel E Wolfram, Mehrabyan S S, Metreveli Z V, Oliveira L C S, Olkiewicz K, Rizatdinova F K, Shabalina EK, Smirnova L N, Tabidze M D, Tikhonova L A, Tomaradze A G, Verbeure F and Zotkin S A 1995 *Z. Phys.* C **66** 385
[13] Ghosh D, Roy J, Sengupta R and Jadavpur U 1987 *Nucl. Phys.* A **470** 683
[14] Ghosh D, Roy J, Sengupta R and Sarker Sh 1992 *Z. Phys.* A **342** 191
[15] Namboodiri M N, Ahle L, Akiba Y, Beavis D, Britt H C, Budick B, Chasman C, Chen Z, Chi C Y, Chu Y Y, Cianciolo V, Cole B A, Costales J B, Crawford H J, Cumming J B, Debbe R, Engelage J, Fung S Y, Gonin M, Gushue S, Hamagaki H, Hansen O, Hayano R S, Hayashi S, Homma S, Kaneko H, Kang J, Kaufman S, Kehoe W L, Kurita K, LeVine M J, Miake Y, Morrison D P, Moskowitz B, Nagamiya S, Nayak T K, Olness J, Remsberg L P, Rothschild P, Sangster T C, Seto R, Dhigaki K, Soltz R, Steadman S G, Stephans G S F, Sung T, Tannenbaum M J, Thomas J, Tonse S, Ueno S, van Dijk J H, Videbaek F, Vossanack O, Wang F Q, Wang Y, Wegner H E, Woodruff D S, Wu Y D, Yagi K, Yang X, Zachary D and Zajc W A 1994 *Nucl. Phys.* A **566** 443c
[16] Abd Allah N N, Mohery M, Zahran E M and Liu F H 2004 *Chin. J. Phys.* **42** 684
[17] Tufail A, Ahmed S and Infar M 1996 *Can. J. Phys.* **74** 141
[18] Bogdonov V G, Perfilov N A, Plyushehev V A and Soloveza Z I 1983 *Yad. Fiz.* **38** 1493
[19] Andreeva N P, Anzon Z V, Bubnov V I, Gaitinov A Sh, Eligbaeva G Zh, Eremenko L E, Kalyachkina G S, Kanygina E K, Chasnikov I Ya, Shakhova Ts I, Gitsok M, Topor V, Khaiduk M, Lepekhin F G, Simonov B B, Vokalova A, Krasnov S A, Tolstov K D, Shabratova G S, Khoshmukhamedov R A, Leskin V A, Salomov D A, Avetyan F A, Marutyan N A, Sarkisova L G, Sarkisyan V R, Vokal S, Karabova M, Silesh E, Totova M, Walter W, Vosek B, Gladysh E, Holynski R, Antonchik V A, Bakaev V A, Bogdanov S D, Ostroumov V I, Bogdanov V G, Plyushchev V A, Solov'eva Z I, Adamovich M I, Larionova V G, Maslennikova N V, Orlova G I, Tret'yakova M I, Kharlamov S P, Chernyavskii M M, Shumbera M, Azimov S A, Abduzhamilov Sh, Abduzhamilov A, Gadzhieva S, Gulamov K G, Zhumanov A, Lukicheva N S, Mirkhodzhaeva D M, Navotnyi V Sh, Petrov V I, Ravvina E A, Saidkhanov N Sh, Svechnikova A N, Chernova L P, Kostanashvili N I, Serdamba L, Togoo R and Tuvdendorzh D 1987 *Yad. Fiz.* **45** 123 (in Russian)
[20] Abd Allah N N, Abou-Steit S A H, Mohery M and Abdel-Aziz S S 2002 *Int. J. Mod. Phys.* E **10** 55
[21] El-Sharkawy S 1994 *Phys. Scr.* **54** 94
[22] Holynski R 1994 *Nucl. Phys.* A **566** 191c
[23] Babecki J and Nowak G 1978 *Act. Phys. Pol.* B **9** 401
[24] Anderson B, Otterlund I and Stenlund E 1978 *Phys. Lett.* B **73** 343
[25] Hegab M K and Hufner J 1981 *Phys. Lett.* B **105** 103
[26] Singh B, Ojha I D and Tuli S K 1994 *Nucl. Phys.* A **570** 819
[27] Jilany M A 1994 *Nucl. Phys.* A **579** 627
[28] Abd-Elhalim S M and Callet A 2003 *Chaos, Solitons and Fractals* **18** 115
[29] Abdelsalam A, Shaat E A, Ali-Mossa N, Abou-Mousa Z, Osman O M, Rashed N, Osman W, Badawy B M and El-Falaky E 2002 *J. Phys.* G **28** 1375
[30] Abd Allah N N 2002 *Int. J. Mod. Phys.* E **11** 105